Angolan Mineral, Oil and Gas Journal 3 (2022) 19–25

Contents lists available at Amogj

Angolan Mineral, Oil and Gas Journal

journal homepage: www.amogj.com

Waterflooding performance evaluation by classical frontal displacement theory

Geraldo Ramos [1, 2]

[1]Research and Development Center of Sonangol, Sonangol EP, Rua Rainha Ginga no 29-31, 1316, Luanda, Angola.

[2]Polytechnic Institute of Technology and Sciences (ISPTEC), Department of Engineering and Technology (DET), Av. Luanda Sul, Rua Lateral Via S10, Talatona, Luanda – Angola.

ARTICLE INFO

Keywords:
Conventional recovery, Waterflood performance, Buckley-Leverett model, Classical frontal advance theory, fractional flow, frontal advance theory

Waterflooding is one of the most successful and widely used techniques to increase oil recovery. This technique is mostly applied to the light and medium oil type once the reservoir's natural drive mechanism is exhausted or the economic limit of the project has been achieved. Several secondary predictions have been developed and are available in the literature. Most of them utilize mathematical correlations and are developed to solve simple problems. Others are for complex problems and depend on numerical simulations or disruptive techniques like artificial intelligence. The effect of oil and water viscosity, dip angle and water injection rate on waterflooding performance using the classical frontal displacement theory developed by Buckley-Leverett has been employed in this study. The horizontal approach is used as base study and two different types of oil (2 cp viscosity and 16 cp) were used. The results show the advance of the injected waterfront are faster on heavy oil than in light oil reservoirs. However, in this case, a significant amount of mobile oil remains behind the waterfront. The cumulative oil production from the light oil at the end of breakthrough is 53% which is 13 % more than that of the heavy oil.

1. INTRODUCTION

Hydrocarbon recovery is at the heart of oil production from underground reservoirs [1,2] and occurs through three main processes: primary oil recovery (natural flow), secondary oil recovery (conventional recovery) and enhanced oil recovery (EOR) also known as tertiary recovery [1–6]. During the primary and secondary recovery stages, mobile oil is easily extracted whereas EOR is adapted properly to extract immobile oil trapped under capillary and viscous forces [6].

Once the primary drive mechanism has been exhausted, the water flooding process is a common and most economically method used to support the reservoir pressure and increase the oil recovery [7]. Although the studies report that the worldwide average oil recovery through waterflooding is 1/3 of the original oil in place, it is widely used to displace oil due to its availability, environmentally friendly, and high efficiency when compared to the primary recovery method or before any other approach such as advanced method has been employed. This is accomplished by *voidage replacement* process which is the injection of water to increase the reservoir pressure to its initial level and maintain it near that pressure [8].

Several factors such as reservoir geometry, fluid properties, reservoir depth, lithology and rock properties, fluid saturations, reservoir uniformity and pay continuity, and primary reservoir-driving mechanisms are essential to determine the suitable candidate for waterflooding operations.

The waterflooding is performed in four different groups of injection patterns. These are the irregular injection patterns, peripheral injection patterns, regular injection patterns, crestal and basal injection patterns [9]. The selection of the suitable flooding patterns depends on the number and location of existing wells. In most cases, producing wells can be converted to injection wells or drilling new injection wells [9].

The waterflooding technique was introduced accidently in 1865 in Pothole, Pennsylvania, by flowing water from a shallow water-bearing layer into the lower oil pay zone [7]. In 1924, the water was first injected by a five-spot pattern in Bradford field [7,8,10,11]. Several analytical models were developed and available in the literature for waterflooding performance. Examples of the common ones and widely used approaches include Dykstra-Parsons, Buckley-Leverett, Craig-Geffen-Morse (CGM), and Stiles.

Dykstra-Parsons developed the approach to predict the performance of waterflooding in noncommunicating stratified reservoirs [11]. The work of Dykstra-Parsons was extended by Reznik in bases of real-time. While Stiles in his studies assumed the displacement velocity in a layer to be proportional to its absolute permeability neglecting the effect of mobility ratio. Hiatt presented a model for communicating layers with complete crossflow [12]. Then, Warren and Cosgrove applied Hiatt's model to stratified systems with a log normal permeability distribution. Another work was reported by Hearn. He presented expressions for the pseudo relative permeability functions for communicating stratified reservoirs [12].

Buckley and Leverett developed a well-known frontal displacement theory [9]. The classical theory consists of two basic equations. Fractional flow equation and frontal advance equation. However, the two approaches are similar in nature but are differentiated by time. However, both characterize the mechanics of oil movement while being displaced from the reservoir by injected fluid.

The frontal advance equation also known as the Buckley-Leverett and Welge tangent method is used to obtain the outlet and average saturations in each layer which is used to obtain the fractional oil recovery and water cut of each layer. Summation over all layers yields the performance of the total system [13]. A frontal displacement theory approach is presented to evaluate the waterflooding performance. The effect of some parameters such as oil and water viscosity, dip angle and injection rate on waterflooding performance are evaluate in this work.

2. ASSUMPTIONS

This study assumes that:

1. The system is linear and of constant thickness.

2. The flow is isothermal, incompressible, and obeys Darcy's law.

3. Capillary forces are negligible.

*Corresponding author. Geraldo Ramos. E-mail: geraldo.ramos@sonangol.co.ao
Received 20 July 2022; Received in revised form 25 July 2022; Accepted 01 July 2022

4. The system is homogeneous with uniform thickness and constant permeability.

5. Porosity characteristics are the same for all systems.

6. The initial fluid saturation is uniform at the irreducible water saturation.

3. METHODOLOGY (MATHEMATICAL MODEL)

The basic equations of the mathematical model and the approaches are presented in this section. The water fractional flow curve and frontal advance approaches are used in this study. These two approaches are well known as classical frontal displacement theory developed by Buckley – Leverett.

3.1. Fractional flow equation

The water fractional flow curve used for the study is derived from two immiscible fluids: oil as displaced fluid and water as displacing fluid and is expressed accord Equation 1.

$$f_w = \frac{q_w}{q_w + q_o} = \frac{q_w}{q_t} \tag{1}$$

At the irreducible (connate) water saturation, the water flow rate is zero (Eq. 1). Therefore, the water cut (f_w) is 0 %. At the residual oil saturation point (S_{or}) the oil flow rate is zero and the water cut reaches its upper limit of 100% [9].

The water flow rate and oil flow rate from the fractional flow equation of water or water cut equation (Eq. 1), can be expressed as:

$$q_w = f_w q_t \tag{2}$$

and

$$q_o = (1 - f_w) q_t \tag{3}$$

Where

$$f_o + f_w = 1 \tag{4}$$

Applying Darcy's law equation, assuming homogeneous system for steady-state flow and combining capillary pressure definition Eq. 1 can be expressed as [9]:

$$f_w = \frac{1 + \left(\frac{k k_{ro} A}{\mu_o q_t}\right)\left[\frac{\partial p_c}{\partial x} - g\Delta\rho \sin(\alpha)\right]}{1 + \frac{k_{ro}}{k_{rw}}\frac{\mu_w}{\mu_o}} \tag{5}$$

In field units, Eq.5 can be expressed as [9]:

$$f_w = \frac{1 + \left(\frac{1.127\times10^{-3} k k_{ro} A}{\mu_o q_t}\right)\left[\frac{\partial p_c}{\partial x} - 0.433 g\Delta\rho \sin(\alpha)\right]}{1 + \frac{k_{ro}}{k_{rw}}\frac{\mu_w}{\mu_o}} \tag{6}$$

Assuming horizontal flow and ignoring capillary pressure gradient, Eq.5 can be expressed as:

$$f_w = \frac{1}{1 + \frac{k_{ro}}{\mu_o}\frac{\mu_w}{k_{rw}}} \tag{7}$$

The given physical properties of the reservoir are used for calculations and the curve of f_w verses S_w is plotted from S_{wi} up to $S_w = 1 - S_{or}$. The plots can also be linked to the given dimensionless water saturation (S_{wD}).

Then, the sensitivity analysis is performed by changing the oil and water viscosity, water injection rate, and horizontality and non-horizontality effect of the reservoir (dip angle concept) on the water fractional flow equation. Equation 3 is used to evaluate the impact of water fractional flow in oil flow rate on waterflooding operation.

3.2 Frontal Advance approach

For frontal advance approach, the tangential points from the initial water saturation are drawn on water fractional flow curve. Then the extended curve from interval of the water saturation at the breakthrough is plotted. The mathematical expression for frontal advance equation can be expressed as [9,14]:

$$x_f = \frac{q_T}{A\Phi}\left(\frac{df_w}{dS_w}\right)_{S_{wf}} \tag{8}$$

Also written as:

$$\frac{x_f}{L} = Q_i(t)\left(\frac{df_w}{dS_w}\right)_{S_{wf}} \tag{9}$$

The tangential points can also be computed mathematically as:

$$\frac{df_w}{dS_w} = \frac{AB[nS_{wD}^{n-1}(1 - S_{wD})^m + mS_{wD}^n(1 - S_{wD})^{m-1}]}{[S_{wD}^n + A(1 - S_{wD})^m]^2} \tag{10}$$

where

$$A = \frac{\alpha_1 \mu_w}{\alpha_2 \mu_o} \tag{11}$$

and

$$B = \frac{1}{1 - S_{or} - S_{wi}} \tag{12}$$

Equation 10 is derived from:

$$f_w = \frac{S_{wD}^n}{S_{wD}^n + S_{wD}^n} \tag{13}$$

Where

$$k_{ro} = \alpha_1(1 - S_{wD})^m \tag{14}$$

$$k_{rw} = \alpha_2 {S_{wD}}^n \tag{15}$$

$$S_{wD} = \frac{(S_w - S_{wi})}{(1 - S_{or} - S_{wi})} \tag{16}$$

The main purpose is to read three main variables by drawing several tangents: water saturation and water fractional flow at breakthrough, and average water saturation at breakthrough($S_{wf}, f_{wf}, \bar{S}_{wf}$). These variables are replaced by S_{w2}, f_{w2}, $\bar{S}_{w2}$.

The pore volume of contacted water can be calculated first with the obtained information, then the time, cumulative oil production, oil flow rate, and water-oil ratio are identified. These equations are described in the next stages of this section.

The cumulative pore volumes injected (PVI) also known as number of waters contacted pore volumes (Q_i) can be calculated as [9,14]:

$$Q_i = \frac{\bar{S}_{wf} - S_{wf}}{1 - f_{wf}} = \frac{\bar{S}_{w2} - S_{w2}}{1 - f_{w2}} \tag{17}$$

The time and cumulative oil production can be expressed as:

$$t = \frac{Q_i \times V_p}{q_t} \tag{18}$$

$$N_p = V_p(\bar{S}_{w2} - S_{wi}) \tag{19}$$

Equation 19 is valid for the values equal and greater of water saturation at breakthrough. At initial water saturation, instead using Eq. 19, is recommended using Eq. 20.

$$N_p = V_p Q_i \tag{20}$$

Oil flow rate is computed using Eq. 3, replacing f_w by f_{w2}. The WOR is computed as:

$$WOR = \frac{f_{w2}}{1 - f_{w2}} = \frac{f_{w2}}{f_{o2}} \tag{21}$$

Oil recovery displacement efficiency (E_D) can be expressed as:

$$E_D = \frac{\bar{S}_{wf} - S_{wi}}{1 - S_{wi}} \tag{22}$$

Time can also be expressed combining Eqs. 17 and 18:

$$t = \left(\frac{\bar{S}_{wf} - S_{wf}}{1 - f_{wf}}\right)\frac{V_p}{q_t} \quad (23)$$

4.0 RESULTS AND DISCUSSION

The oil and water relative permeabilities relations used in this study are:

$$k_{ro} = (1 - S_{wD})^{2.56} \quad (24)$$

$$k_{rw} = 0.78 S_{wD}{}^{3.72} \quad (25)$$

The relation for S_{wD} is represented using Eq. 16. The reservoir is narrow "shoestring" with porosity of 15% and formation-volume factor for both oil and water is 1.0. Water injection rate of 338 B/D. The other parameters are listed in Table 1

Table 1: Rock and fluid physical proprieties. Adapted from [9]

Parameter	Value	Parameter	Value
Porosity	0.15	Oil viscosity	2.0 cp
Thickness	20 ft	Initial Water Saturation	0.363
Water viscosity	1.0 cp	Residual oil saturation	0.205
Permeability	100 md	Wellbore radius	0.5 ft
Oil density	45 lb/ft^3	Water density	64 lb/ft^3
Angle	20º	Length	1000 ft
Width	300 ft		

Figure 1 shows the dimensionless water saturation as a function of both water and oil permeability. The saturation points of intersection between K_{ro} and K_{rw} is greater than 50%. This represents the typical water-wet reservoir structure.

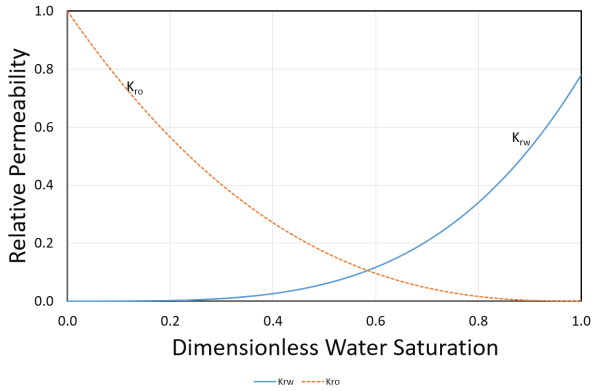

Figure 1: Water-wet reservoir relative permeability as a function of dimensionless water saturation.

Water and oil flow during waterflooding operations. Oil flows through the largest pores spaces with high value of oil relative permeability. In a reservoir system with oil and water, it is well known that:

$$S_o + S_w = 1 \quad (26)$$

This implies that if water saturation increases, oil saturation decreases, thus, oil relative permeability decreases. During water injection process, while oil moves from the smaller to larger pore spaces, the throats formally filled with oil are replaced by water.

Once the pressure is not sufficient to overcome the viscous and capillary pressure for the water saturated pore throat, this leads to a trapped oil in place [13]. The water fills-up the continuous flow paths and oil stops flowing (trapped in large pores). This trapped oil is one target of enhanced oil recovery methods.

The plot of saturation vs water cut is S – shaped, as shown in Figure 2. The limits of the f_w curve (0 and 1) are defined by the end points of the relative permeability curves.

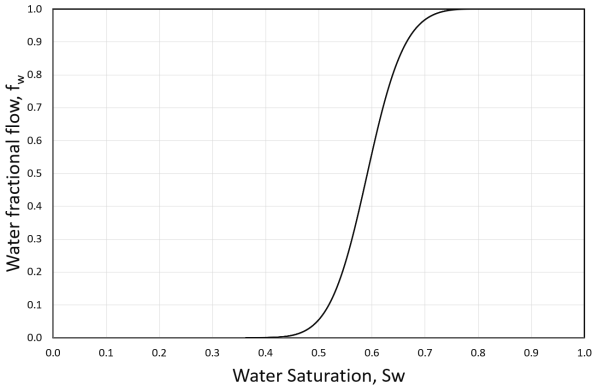

Figure 2: Water fractional flow (water cut) curve vs saturation

During oil displacement by water injection (waterflood), an increase in f_w at any point in the reservoir, causes a proportional decrease in f_o and oil mobility (Eq. 4 and Figure 3).

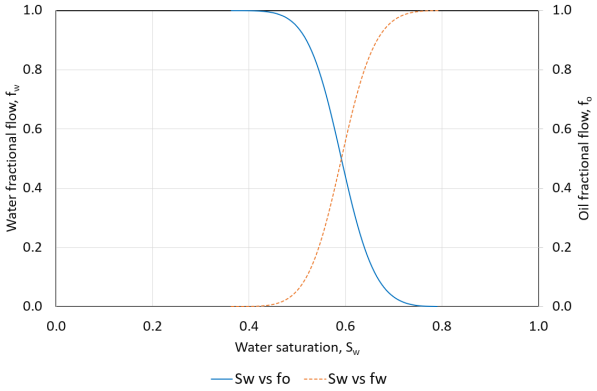

Figure 3: Behaviour of Oil and water fractional flow curves in term of water saturation.

Therefore, it is crucial to select a suitable injection scheme in waterflooding operations that reduces the fractional flow of water. To reduce the negative effect of water cut, some parameters such as viscosity of the injected water, formation dip angle, and water injected rate on the water cut must be investigated. The overall effect of these parameters on the water fractional flow curve are discussed next.

4.1 The effect of viscosity on f_w and q_o curves

Capillary pressure gradient and gravity effect are ignored in this approach. This implies using Eq.7. The analysis shows that, the higher injected water viscosities, the higher the value of the denominator, leading to overall fractional flow decrease. This is illustrated in Figure 4 with downward shift of the curves.

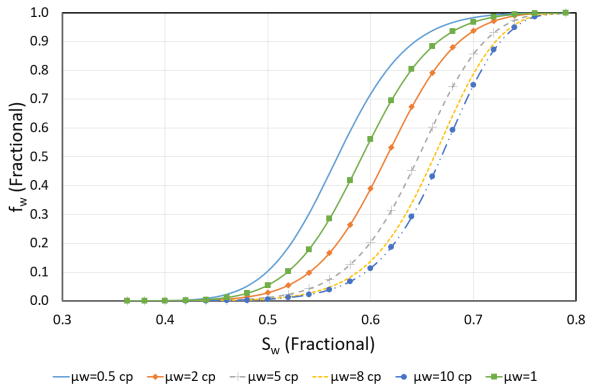

Figure 4: The effect of water viscosity on water cut (f_w).

The reduction of water cut, increases the oil flow rate in waterflooding operations. This is illustrated in Figure 5 using Eq. 3. For example, the injected water viscosity of 10 cp (the highest used in this analysis) is shifted to the right meaning more oil displacement compared to the others tested in this study. Increasing oil recovery by water cut reduction is a requirement for successful water flooding operations.

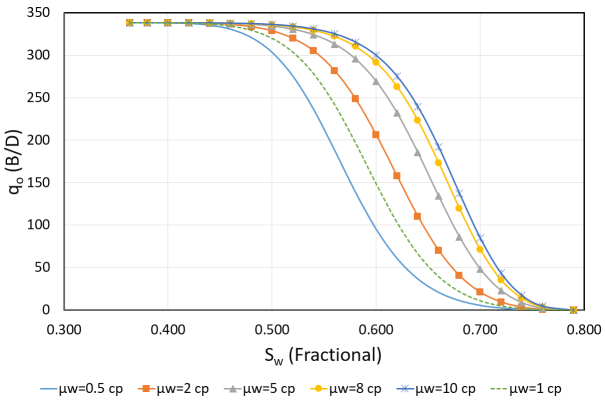

Figure 5: Effect of water injected viscosity in oil flow rate

The effect of oil viscosity on water cut is also investigated in this study. The result illustrates that, a higher oil viscosity results in an increase (an upward shift) in the fractional flow curve (Figure 6).

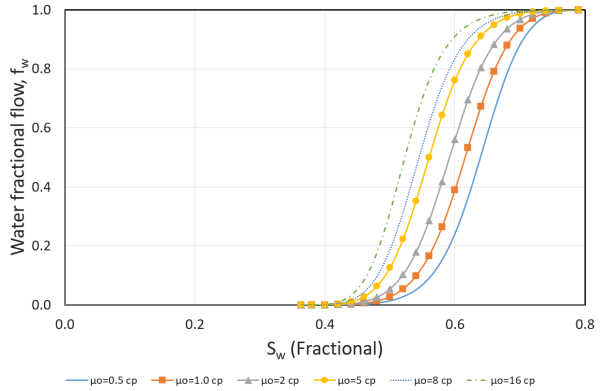

Figure 6: The effect of oil viscosity on water cut (f_w)

The water fractional flow curve of light oil showed a regular S-shape. The application of this curve to the waterflooding method showed that a large amount of mobile oil in the reservoir is displaced by water injection. In contrast, the fractional flow curve of heavy oil did not display an S-shape because of its high viscosity, and a significant amount of mobile oil remains in the reservoir behind the waterfront.

4.2 The effect of dip angle on water fractional flow (f_w)

The effect of dip reservoir angle on water fractional flow curve is evaluated in this section. According to the given physical data (Table 1) of the field, knowing that for the updip displacement *sin* (α) is positive, then from Eq. 6 can be expressed:

$$f_w = \frac{1 - 4.787 k_{ro}[\sin(\alpha)]}{1 + 0.5\left(\frac{k_{ro}}{k_{rw}}\right)} \quad (27)$$

Alternatively, for downdip displacement where *sin* (α) is negative:

$$f_w = \frac{1 + 4.787 k_{ro}[\sin(\alpha)]}{1 + 0.5\left(\frac{k_{ro}}{k_{rw}}\right)} \quad (28)$$

The result is plotted in Figure 7 for both 20 degrees downdip and updip angle. The updip flow represents the oil updip is displaced by water. The injection well is located downdip and more efficient performance is reached. The *sin* (α) is positive, and numerator will always remain negative. This effect leads to a downward shift of the water fractional flow curve (decrease of f_w curve) [9].

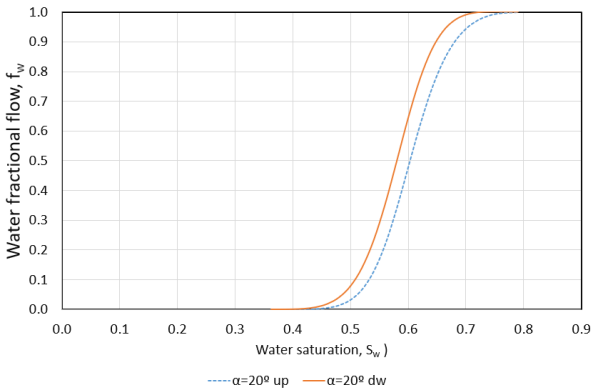

Figure 7: Effect of dip angle on water cut, f_w.

Since the downdip the *sin* (α) is negative, the numerator of Eq.6 will always remain positive. The oil is displaced downdip. In this case, the injection well is located updip, which causes an increase in the f_w curve (upward shift). This scenario is beneficial when injection wells are located at the top of the structure. The water is injected at a higher injection rate to improve the displacement efficiency [9].

The sensitivity analysis is performed assigning the value of the angle to 5, 10, 15, and 20 degrees for both updip and downdip. The result is depicted in Figure 8.

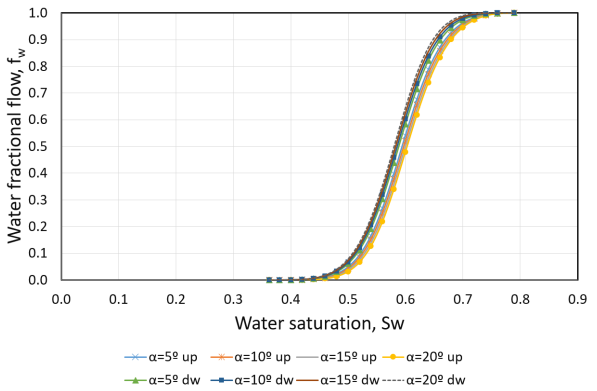

Figure 8. Sensitive analysis of the effect of the dip angle on water fractional flow curve

From the Figure 8, for the updip displacement, the higher the angle, the water fractional flow curve shifts to the right. This action is inverse to the downdip displacement flow.

It is important to recall that the possibility exists for the cases of f_w being greater than one. This phenomenon is known as counterflow. This occurs when displacing the oil downdip at a low water injection rate. The oil phase is moving in a direction opposite to that of the water. Oil is moving upward and the water downward [9].

The other case that the water fractional flow curve is greater than one is when the water-injection wells are located at the top of a tilted formation. The injection rate must be high to avoid oil migration to the top of the formation. So, in this case water fractional flow curve is greater than one [14].

4.3 The effect of Injection rate on water fractional flow

For horizontal reservoir or the cases that the dip angle is zero, the injection rate has no effect on the fractional flow curve (Eq. 7).

The injection rate was evaluated by changing the given total pumping rate of 338 B/D to 1000 B/D, 2000 B/D, 3000 B/D, and 4000 B/D. The result of the study is illustrated in Figure 9. Thus, the higher the total water injection rate, the more the curve is shifted to the left. The smaller the total injection rate, the more the curve is shifted to the right.

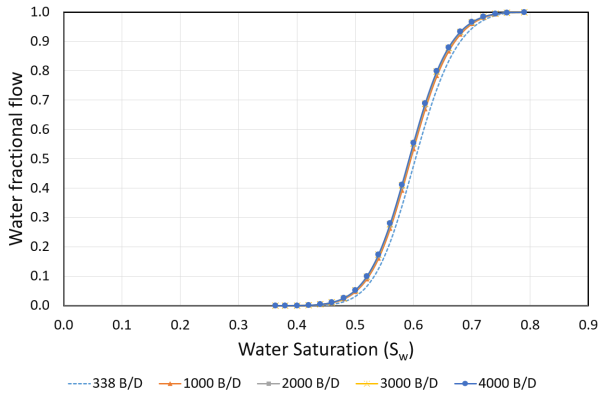

Figure 9: The effect of water injection rate on water fractional flow curve

This shows that the higher the injection rate the higher the water fractional flow curve. Then, designing a suitable injection rate is crucial in waterflooding operations. The main purpose of these operations is in reducing the water cut and increase the oil production.

Frontal Advance approach of Buckley-Leverett is presented to evaluate the displaced oil in reservoir. The water fractional flow curve versus saturation of the given data (Table 1) is presented in Figure 10. The tangential linear curve is plotted from the initial water saturation.

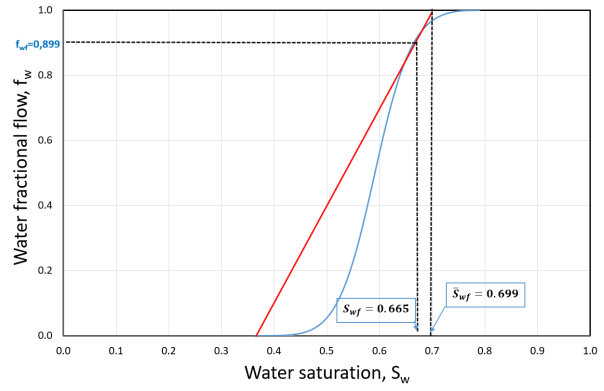

Figure 10: Fractional flow curve with tangent drawn to find water saturation at breakthrough (S_{wf}) for the given data (light oil).

The point of tangency defines the breakthrough or flood front saturation, S_{wf}. Saturations greater than S_{wf} satisfy the Eq. 7, in contrast to fractional flows for saturations less than S_{wf} that do not satisfy [15].

From Figure 10, the flood front saturation or water saturation at breakthrough (S_{wf}) is 0.665 and the average water saturation at breakthrough ($\bar{S}_{wf}$) is 0.669. If the tangent construction is correct, the values of Qi from Eq. 17 and Eq. 29 will be the same [14].

$$Q_i = \bar{S}_{wf} - S_{wi} \qquad (29)$$

If the values are different, a trial-and-error procedure is used to find the $\bar{S}_{wf}$ that satisfies both equations [14].

This step requires zooming the plot from Figure 10 within the intervals water saturation at breakthrough (S_{wf}). The performance after breakthrough is determined by selecting values of water saturation greater than 0.665, S_{wf}, (replaced by S_{w2}) and determining f_{w2} and f_{w2}' for each S_{w2} by drawing tangents to expanded fractional flow curve. Figure 11 is an example of reading one point from the expanded plot.

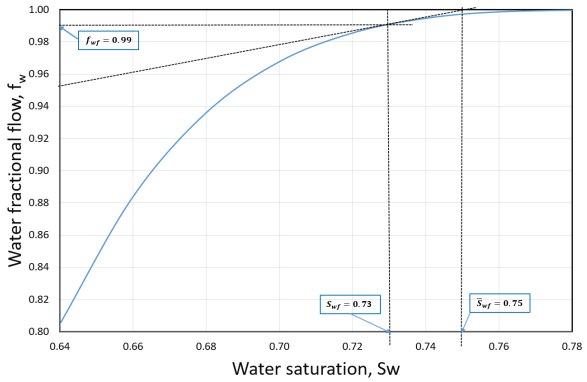

Figure 11: Expanded water fractional flow curve and extrapolation of the tangent to fractional flow curve for computation of performance after breakthrough

Using the approach of Figure 10, the values of water saturation and water fractional flow after breakthrough, are determined from the tangent line (Figure 11). These values can be replaced by S_{w2}, f_{w2}, $\bar{S}_{w2}$ as described in the previous section. Each saturation advances into the system at a rate in direct proportion to df_w/dS_w.

The results of the calculated saturation profile for given oil viscosity (a light oil reservoir) are illustrated in Figure 12. The saturation front from the plot moves with a constant speed toward the production site. Although there is a large amount of residual oil in the reservoir, water displaces most of the mobile oil [16].

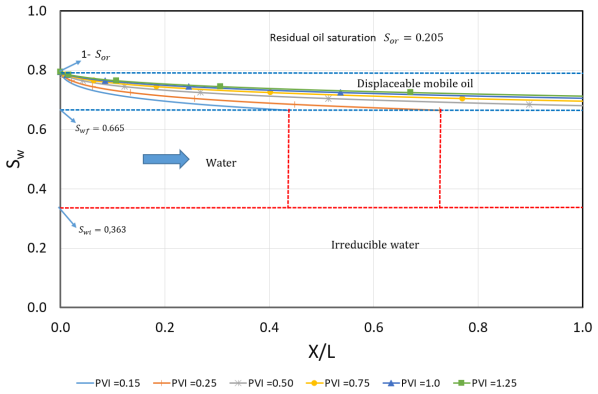

Figure 12: Displacement of light oil calculated by the frontal advance equation.

The equations 17 – 19 are used to compute the quantity of water contacted pore volumes (Q_i), the time and cumulative oil production. The oil flow rate is estimated using Eq.3.

The plot illustrated in Figure 13 is the oil flow rate and cumulative oil production as a function of time. The sharp drop of oil flow rate curve represents a breakthrough time of the reservoir. Since flow rate is related to water cut (f_w) Eq. 3, the frontal advance solution drops the fractional flow of oil at the point of breakthrough from 1 to 1 – f_{swf}.

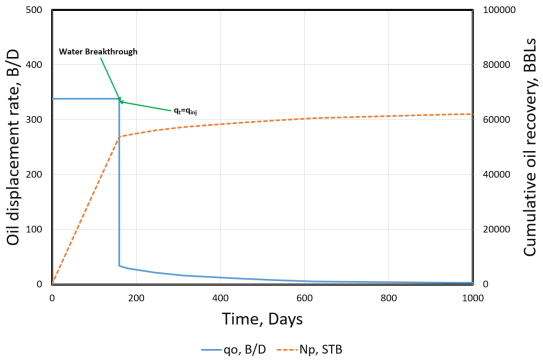

Figure 13: Displacement from frontal advance solution.

Cumulative oil production at the breakthrough can be estimated using Eq. 10:

$$N_p = \frac{300\times1000\times20\times0.15(0.699-0.363)}{5.615}$$

$$N_p = 53\,856\ BBls$$

The time to reach the breakthrough is estimated using Eq.23:

$$t_{BT} = \left(\frac{\bar{S}_{wf} - S_{wf}}{1-f_{wf}}\right)\frac{V_p}{q_t}$$

$$t_{BT} = \left(\frac{0.699-0.665}{1-0.899}\right)\frac{300\times1000\times20\times0.15}{338\times5.615}$$

$$t_{BT} = 159.6\ days$$

From Eq. 22, using data from Figure 10 and the given physical values (Table 1), the estimated displacement efficiency (E_D) of the reservoir is 0.53, or:

$$E_D = \frac{0.699-0.363}{1-0.363} = 0.53$$

The graph of displacement efficiency for the investigated reservoir as a function of time and at different average water saturation is depicted in Figure 14. This plot illustrates the increase of oil displaced as the time progresses.

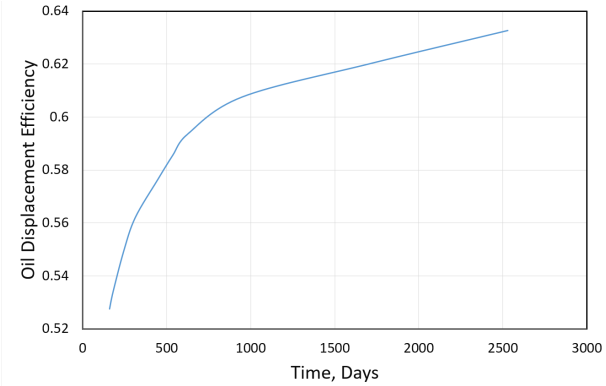

Figure 14: Oil displacement of the investigated reservoir versus time.

A decrease on oil saturation was observed when there is an increase in the number of water contacted pore volumes. This is illustrated in Figure 15. The water injected fills up the volume of pores displacing the oil.

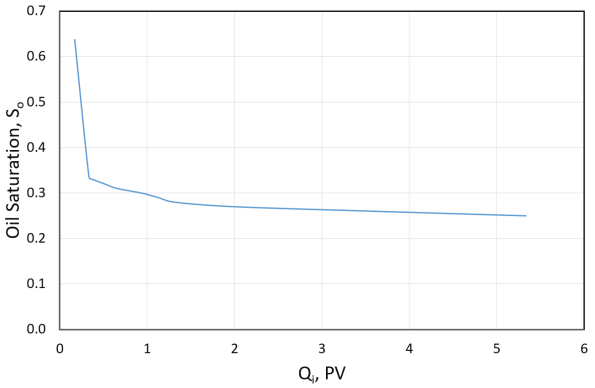

Figure 15: Oil saturation versus the number of waters contacted pore volumes

An additional study was performed for heavy oil (16 cp) with frontal advance equation. The water saturation profile was calculated and plotted with different pore volume of contacted water. The results presented a significant amount of mobile oil remains in the reservoir after displacement (Figure 16).

However, the effective saturation for this displacement is larger than that for light oil [16]. This type of oil requires additional action, thermal Enhanced Oil Recovery (thermal EOR) to displace the immobile oil trapped in the reservoir by capillary and viscous forces.

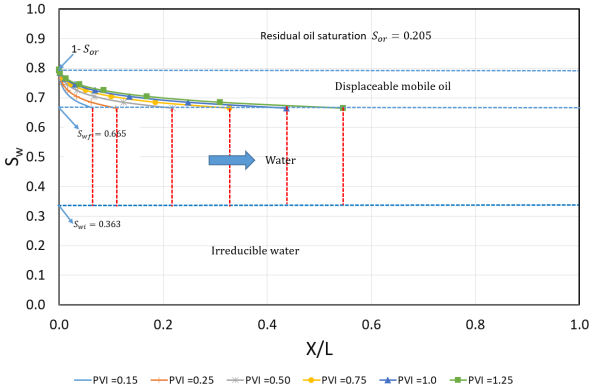

Figure 16: Displacement of heavy oil calculated by the frontal advance equation.

The drawn tangent of water fractional curve for heavy oil (16 cp) is illustrated in Figure 17. The computed cumulative oil production at breakthrough is 41 193 BBLs, while time to reach the breakthrough is estimated to be 126.5 days. The displacement efficiency of the evaluated heavy oil is 0.40 or 40%.

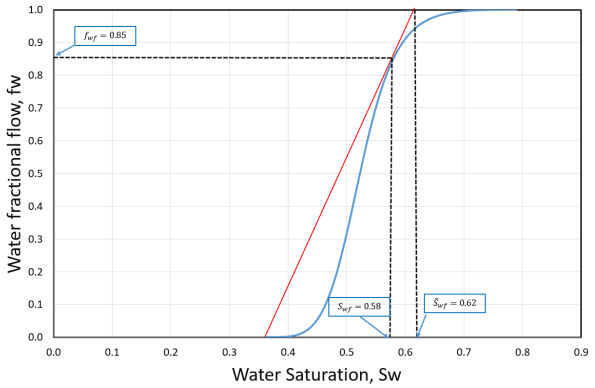

Figure 17: Fractional flow curve with tangent drawn to find water saturation at breakthrough (S_{wf}) for heavy oil (16 cp).

Table 2 summarizes the computed values of both light and heavy oil. The studies illustrated that in light oil case, the advance of the waterfront for the heavy oil reservoir is faster than that for the light oil reservoir. These results are reflected in the shape of the fractional flow curve of the reservoir oil (Figure 10 and 17) or from the value of breakthrough time as illustrated in Table 2.

The cumulative production at breakthrough is approximately 23.5% more from the oil with 2 cp viscosity compared to the oil of 16 cp viscosity.

Table 2: Summary oil displacement for light and heavy oil

Oil Type	Viscosity, cp	Displacement Efficiency, %	Cumulative Oil Production, BBls	Breakthrough Time, days
Light Oil	2	53%	53 856	159.6
Heavy	16	40%	41 193	126.5

Conclusions

The effect of water viscosity, oil viscosity, and dip displacement angle on waterflooding performance was evaluated using the classical frontal displacement theory. The horizontal fractional water flow was deeply investigated and used as the base case of this study. The displacement efficiency of the investigated light oil is 13% more than the value observed from the heavy oil. Water injection has no effect for the horizontal water fractional flow curve once the capillary and gravitational forces are ignored for this case. While for no horizontal case, the higher the angle, the water fractional flow curve shifts to the right in contrast to the downdip displacement flow, which shifts to the left.

Nomenclature

A = cross-sectional area
E_D = displacement efficiency
f_o = oil fractional flow
f_{o2} = oil fractional flow at position x_2
f_{swf} = water fractional flow at breakthrough
f_w = water cut or water fractional flow, dimensionless
f_{w2} = water fractional flow at position x_2
g = gravity constant
k = absolute permeability
k_{ro} = relative permeability to oil
k_{rw} = relative permeability to water
L = length
N_p = cumulative oil production
N_{pbt} = cumulative oil production at breakthrough
p_c = capillary pressure
Q_i = cumulative pore volumes injected, or number of waters contacted pore volumes
q_o = oil production rate
q_t = total flow rate, total injection rate or total production rate
q_T = total pumping rate of oil and water
q_w = water production rate
S_o = oil saturation
S_{or} = residual oil saturation, fraction
S_w = water saturation
S_w = water saturation, fraction
S_{wD} = dimensionless water saturation
S_{wf} = water saturation at breakthrough, fraction
S_{wi} = initial water saturation, fraction
$\bar{S}_{wf}$ = average water saturation at breakthrough, fraction
V_p = pore volume
X_f = dimensionless distance of the displacement front
α = dip angle
Δρ = water – oil density differences
μ_o = oil viscosity
μ_w = water viscosity
ρ_o = oil density
ρ_w = water density
Φ = porosity, fraction

Acknowledgement

Thanks to Mrs. Karen Winfrey and other reviewers, for their comments that helped to improve the manuscript.

Conflict of interest

The authors declare that there is no conflict of interest regarding the publication of this manuscript.

References

[1] Sunil Kokal and Abdulaziz Al-Kaabi. Enhanced oil recovery: challenges and opportunities. World Petroleum Council, pages 64–69, 2010.

[2] Ramos, G. A. R., & Yates, K. (2021). Enhanced Oil Recovery: Projects Planning Strategy in Angolan Oilfields. Angolan Mineral, Oil & Gas Journal, 2(2), 1-11.

[3] George J. Stosur. EOR: Past, present and what the next 25 years may bring. SPE 84864, October 2003.

[4] George J. Stosurand J. Roger Hite, Norman F. Carnahan, and Karl Miller. The alphabet soup of IOR, EOR and AOR: Effective communication requires a definition of terms. SPE 84908, October 2003.

[5] Laura Romero-Zerón, editor. Introduction to Enhanced Oil Recovery (EOR) Processes and Bioremediation of Oil Contaminated Sites. ISBN 978-953-51-0629-6. InTech, Janeza Trdine 9, 51000 Rijeka, Croatia, May 2012.

[6] Tarek Ahmed and Nathan Meehan. Advanced Reservoir Management and Engineering. ISBN: 978-0-1238-5548-0. Gulf Professional Publishing is an imprint of Elsevier, 2nd edition, October 2012.

[7] Ali, J. A., & Stephen, K. (2018). A semi-analytical method for history matching and improving geological models of layered reservoirs: CGM analytical method. Journal of Chemical and Petroleum Engineering, 52(1), 69-80.

[8] PetroWiki. Waterflooding. << https://petrowiki.spe.org/Waterflooding>>. Consulted on February, 02, 2022.

[9] Ahmed, T. (2018). Reservoir engineering handbook. Gulf professional publishing.

[10] Fettke, C. R. (1938). The Bradford oil field Pennsylvania and New York (No. TN873. F47 1938.).

[11] Craig, F. (1971). "The reservoir engineering aspects of waterflooding." 1st ed., New York: Hen-ry L, Doherty Memorial Fund of AIME.

[12] El-Khatib, N. A. (2012). The modification of the Dykstra-parsons method for inclined stratified reservoirs. SPE Journal, 17(04), 1029-1040.

[13] El-Khatib, N. A. (2001, March). The application of Buckley-Leverett displacement to waterflooding in non-communicating stratified reservoirs. In SPE Middle East Oil Show. OnePetro.

[14] Willhite, G. P. (1986). Waterflooding. Society of petroleum engineers, Richardson, TX

[15] Abdallah, W., Buckley, J. S., Carnegie, A., Edwards, J., Herold, B., Fordham, E., ... & Ziauddin, M. (1986). Fundamentals of wettability. Technology, 38(1125-1144), 268.

[16] Nazari, A. J., Nasiry, A. F., & Honma, S. (2016). Effect of fractional flow curves on the recovery of different types of oil in petroleum reservoirs. Proc. Schl. Eng. Tokai Univ., Ser E, 41, 53-58.